Non-reflecting boundary conditions and domain decomposition methods for industrial flow acoustics

Philippe Marchner

University of Lorraine, University of Liège

Soutenance de thèse
Nancy, June 16th, 2022

X. Antoine | C. Geuzaine | H. Bériot/P. Barabinot

Outline

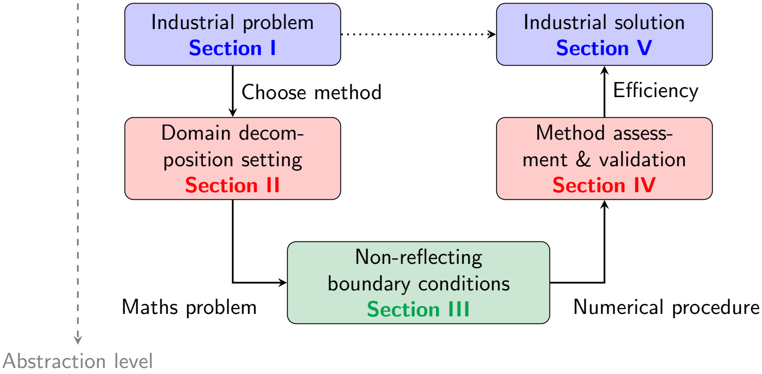
Industrial problem
Section I
Industrial solution
Section V
Choose method
Efficiency
Domain decom-position setting
Section II
Method assess-ment & validation
Section IV
Non-reflecting boundary conditions
Section III
Maths problem
Numerical procedure
Abstraction level

Outline

Industrial context

Long term perspective

Predict noise from bodies in motion for the transport industry

Computational (aero)acoustics

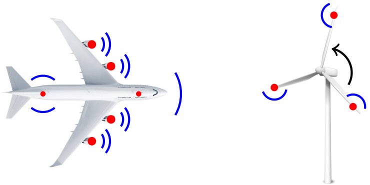

1. analyze & extract sources
2. understand sound propagation
3. find solutions (new material or design)

Industrial objective

Provide a "*ready-to-use*" sound propagation simulation tool

- suitable to modern computer architectures
- applicable to large, complex industrial problems

→ can serve as basis for optimization routines

Outline

Physical models for sound propagation

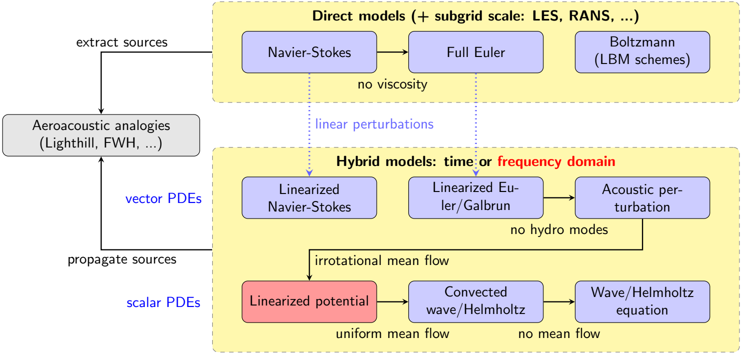

Hybrid model - solve mean flow and acoustic perturbations separately

- we choose the **time-harmonic Linearized Potential Equation**
- simple but accurate for single tones of turbofan engine intakes

Physical model - Linearized Potential Equation

Scalar equation for the acoustic velocity potential $\boldsymbol{v} = \nabla u$

Linearized Potential Equation (LPE)

$$\rho_0(\boldsymbol{x}) \frac{\mathrm{D}_0}{\mathrm{D}t} \left(\frac{1}{c_0(\boldsymbol{x})^2} \frac{\mathrm{D}_0 u}{\mathrm{D}t} \right) - \nabla \cdot (\rho_0(\boldsymbol{x}) \nabla u) = f, \quad \frac{\mathrm{D}_0}{\mathrm{D}t} = \mathrm{i}\omega + \boldsymbol{v}_0(\boldsymbol{x}) \cdot \nabla$$

Helmholtz-type problem with convection and heterogeneities

Mathematical difficulties

- oscillatory, non-local solution
- complex valued, strongly indefinite with ω
- unbounded domain
- convection effects

does not converge with classical iterative methods [*Ernst, Gander 2012*]

→ use a **direct solver**

Point source in a uniform flow

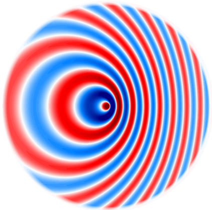

$\mathrm{M} = \|\boldsymbol{v}_0\| / c_0 = 0.6$
$\mathrm{M} < 1$ (Subsonic flow)

Outline

Industrial example : single tone turbofan intake radiation
Current solver : high-order *p*-FEM with direct solver (`MUMPS`)

$\omega_{\text{bpf}} \leftrightarrow \approx 25$ wavelengths

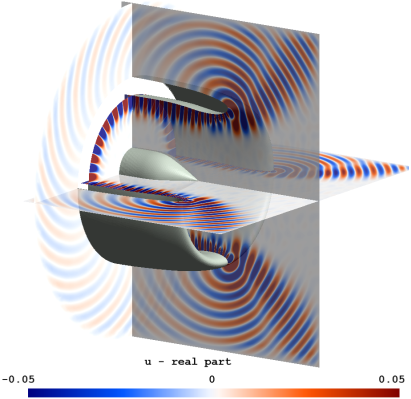

ω_{bpf}, $N_{\text{dofs}} = 10\text{M}$, nnz $= 730\text{M}$
Direct solver $\rightarrow$ 740 Gb of RAM

$\Downarrow$ increase ω ?

$2 \times \omega_{\text{bpf}}$, $N_{\text{dofs}} = 73\text{M}$, nnz $= 5\text{B}$
Direct solver $\approx$ 6 Tb of RAM ...

$\mathcal{O}(\omega^3)$ scaling in memory & time ...

can we distribute the memory cost ? $\rightarrow$ domain decomposition

Outline

Objective of the thesis

Industrial objective

Provide a (scalable) parallel solver to increase the upper frequency limit

Starting point of the thesis

Discretization

- high-order finite elements
  $\rightarrow$ reduce discretization error (interpolation & dispersion)
- adaptive order based on *a-priori* error indicator [*Bériot et al. 2016*]
  $\rightarrow$ less unknowns

Parallelization

- algebraic parallelization is hard for Helmholtz problems
- instead, "divide and conquer" at the continuous (PDE) level
  $\rightarrow$ domain decomposition
- lots of approaches, but common framework [*Gander, Zhang 2019*]

Selected solution - 1st objective

Extend the non-overlapping optimal Schwarz domain decomposition framework [*Boubendir et al. 2012*] to the Linearized Potential Equation

Outline

Outline

Overview - Non-overlapping optimal Schwarz

Toy example: disk scattering by a plane wave

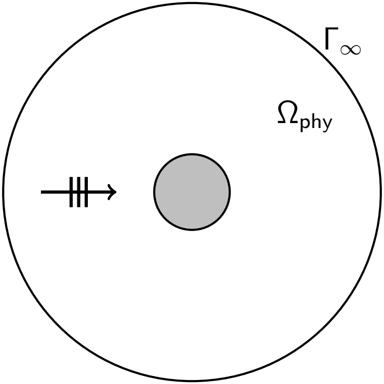

Overview - Non-overlapping optimal Schwarz

Toy example: disk scattering by a plane wave

- Partition $\Omega = \bigcup_{i=0}^{N_{\mathrm{dom}}-1} \Omega_i$ into subdomains

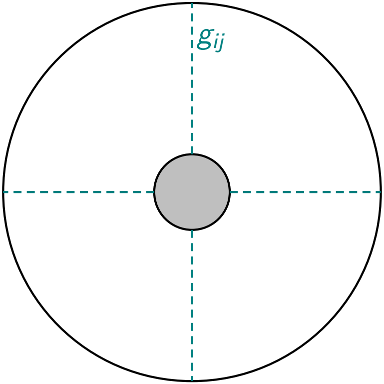

Overview - Non-overlapping optimal Schwarz

Toy example: disk scattering by a plane wave

- Partition $\Omega = \bigcup_{i=0}^{N_{\text{dom}}-1} \Omega_i$ into subdomains

Iterate until convergence

1. Solve the volume subproblems u_i with boundary conditions

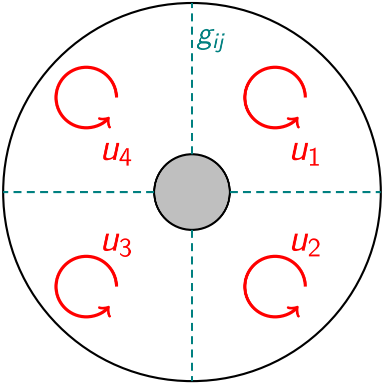

Overview - Non-overlapping optimal Schwarz

Toy example: disk scattering by a plane wave

- Partition $\Omega = \bigcup_{i=0}^{N_{\text{dom}}-1} \Omega_i$ into subdomains

Iterate until convergence

1. Solve the volume subproblems u_i with boundary conditions
2. update the interfaces unknowns $\boldsymbol{g} = (g_{ij}, g_{ji})$ through transmission conditions $(\mathcal{S}_i, \mathcal{S}_j)$ $\Leftrightarrow$ solve surface problem

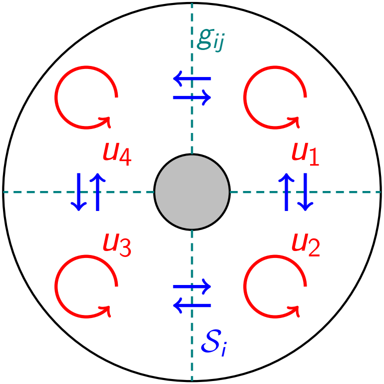

Overview - Non-overlapping optimal Schwarz

Toy example: disk scattering by a plane wave

- Partition $\Omega = \bigcup_{i=0}^{N_{\text{dom}}-1} \Omega_i$ into subdomains

Iterate until convergence

1. Solve the volume subproblems u_i with boundary conditions
2. update the interfaces unknowns $\boldsymbol{g} = (g_{ij}, g_{ji})$ through transmission conditions $(\mathcal{S}_i, \mathcal{S}_j) \Leftrightarrow$ solve surface problem

  - convergence ? [*Després 1991*]
  - How to choose the operators $(\mathcal{S}_i, \mathcal{S}_j)$? $\rightarrow$ *numerous works ...*

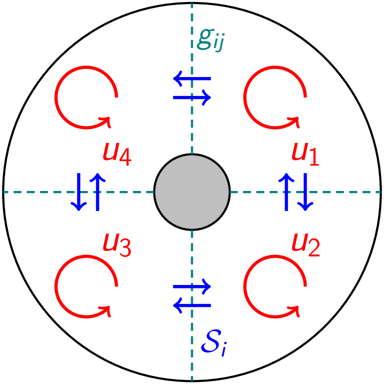

Optimal convergence with the **Dirichlet-to-Neumann** operator

Outline

Flow acoustics formulation

In each subdomain Ω_i, solve the boundary value problems

Non-overlapping optimal Schwarz formulation

$$\begin{cases} \rho_0 \frac{D_0}{Dt}\left(\frac{1}{c_0^2}\frac{D_0 u_i}{Dt}\right) - \nabla\cdot(\rho_0 \nabla u_i) = 0 \text{ in } \Omega_i, \text{ (LPE)} \\ \rho_0\left(1-M_{\boldsymbol{n}}^2\right)\left(\partial_{\boldsymbol{n}_i} u_i + \imath \widetilde{\Lambda}^+ u_i\right) = 0, \text{ on } \Gamma_i^\infty \text{ (radiation condition)} \\ \rho_0\left(1-M_{\boldsymbol{n}}^2\right)\left(\partial_{\boldsymbol{n}_i} u_i + \imath \mathcal{S}_i u_i\right) = g_{ij}, \text{ on } \Sigma_{ij}, \text{ (interface condition)} \end{cases}$$

Introduce the interface coupling on Σ_{ij}

$$\begin{aligned} g_{ij} &= \rho_0\left(1-M_{\boldsymbol{n}}^2\right)\left(-\partial_{\boldsymbol{n}_j} u_j + \imath \mathcal{S}_i u_j\right) \\ &= -g_{ji} + \imath\rho_0\left(1-M_{\boldsymbol{n}}^2\right)(\mathcal{S}_i + \mathcal{S}_j)u_j := \mathcal{T}_{ji} g_{ji} + b_{ji} \end{aligned}$$

Rewrite the coupling as a linear system for $\boldsymbol{g} = (g_{ij}, g_{ji})^T$

$$\underbrace{(\mathcal{I}-\mathcal{A})}_{\text{iteration matrix}} \underbrace{\boldsymbol{g}}_{\text{interface unknowns}} = \underbrace{\boldsymbol{b}}_{\text{physical sources}}, \quad \mathcal{A} = \begin{pmatrix} 0 & \mathcal{T}_{ji} \\ \mathcal{T}_{ij} & 0 \end{pmatrix}$$

$\mathcal{T}_{ij}$ and $\mathcal{T}_{ji}$ are the iteration operators, and can be written in terms of $\widetilde{\Lambda}^+$

High-level algorithmic procedure

Surface iteration operators

$$\mathcal{T}_{ji} = \frac{\mathcal{S}_i - \widetilde{\Lambda}^+}{\mathcal{S}_j + \widetilde{\Lambda}^+}, \quad \mathcal{T}_{ij} = \frac{\mathcal{S}_j + \widetilde{\Lambda}^-}{\mathcal{S}_i - \widetilde{\Lambda}^-}$$

Iteration matrix eigenvalues: $\lambda_{(\mathcal{I}-\mathcal{A})} = 1 \pm \sqrt{\mathcal{T}_{ji}\mathcal{T}_{ij}}$

If we choose $\mathcal{S}_i = \widetilde{\Lambda}^+$ and $\mathcal{S}_j = -\widetilde{\Lambda}^-$, we have optimal convergence

Parallel iterative algorithm for the process i

Do in Ω_i at iteration $(n+1)$, $\forall j \in D_i$

1. given $g_{ij}^{(n)}$, solve $u_i^{(n+1)}$ in Ω_i,
2. update the $(n+1)$ neighbourhood data through $g_{ji}^{(n+1)} = -g_{ij}^{(n)} + \imath\rho_0 \left(1 - M_{\boldsymbol{n}}^2\right) (\mathcal{S}_i + \mathcal{S}_j) u_i^{(n+1)}$ on Σ_{ij},

High-level algorithmic procedure

Surface iteration operators

$$\mathcal{T}_{ji} = \frac{\mathcal{S}_i - \widetilde{\Lambda}^+}{\mathcal{S}_j + \widetilde{\Lambda}^+}, \quad \mathcal{T}_{ij} = \frac{\mathcal{S}_j + \widetilde{\Lambda}^-}{\mathcal{S}_i - \widetilde{\Lambda}^-}$$

Iteration matrix eigenvalues: $\lambda_{(\mathcal{I}-\mathcal{A})} = 1 \pm \sqrt{\mathcal{T}_{ji}\mathcal{T}_{ij}}$

If we choose $\mathcal{S}_i = \widetilde{\Lambda}^+$ and $\mathcal{S}_j = -\widetilde{\Lambda}^-$, we have optimal convergence

Parallel iterative algorithm for the process i

Do in Ω_i at iteration $(n+1)$, $\forall j \in D_i$

1. given $g_{ij}^{(n)}$, solve $u_i^{(n+1)}$ in Ω_i,
2. update the $(n+1)$ neighbourhood data through $g_{ji}^{(n+1)} = -g_{ij}^{(n)} + \imath\rho_0 \left(1 - M_{\boldsymbol{n}}^2\right) (\mathcal{S}_i + \mathcal{S}_j) u_i^{(n+1)}$ on Σ_{ij},

$(\widetilde{\Lambda}^+, -\widetilde{\Lambda}^-)$ are **non-local** DtN maps for the LPE

$\rightarrow$ design **sparse approximations** $\mathcal{S}_i \approx \widetilde{\Lambda}^+$ and $\mathcal{S}_j \approx -\widetilde{\Lambda}^-$

$\Leftrightarrow$ approximate Schur complements at the algebraic level

Algebraic interpretation of domain decomposition

Global problem for two subdomains (i, j) with a common interface Σ

$$\begin{pmatrix} \mathbb{K}_i^{\Omega} & 0 & \mathbb{K}_i^{\Omega,\Sigma} \\ 0 & \mathbb{K}_j^{\Omega} & \mathbb{K}_j^{\Omega,\Sigma} \\ \mathbb{K}_i^{\Sigma,\Omega} & \mathbb{K}_j^{\Sigma,\Omega} & \mathbb{K}_i^{\Sigma,\Sigma} + \mathbb{K}_j^{\Sigma,\Sigma} \end{pmatrix} \begin{pmatrix} u_i^{\Omega} \\ u_j^{\Omega} \\ u^{\Sigma} \end{pmatrix} = \begin{pmatrix} f_i^{\Omega} \\ f_j^{\Omega} \\ f_i^{\Sigma} + f_j^{\Sigma} \end{pmatrix}$$

Direct parallel solver $\rightarrow$ block LU factorization per subdomain

$$\begin{pmatrix} \mathbb{I} & 0 & 0 \\ 0 & \mathbb{I} & 0 \\ \mathbb{K}_i^{\Sigma,\Omega}(\mathbb{K}_i^{\Omega})^{-1} & \mathbb{K}_j^{\Sigma,\Omega}(\mathbb{K}_j^{\Omega})^{-1} & \mathbb{I} \end{pmatrix} \begin{pmatrix} \mathbb{K}_i^{\Omega} & 0 & 0 \\ 0 & \mathbb{K}_j^{\Omega} & 0 \\ 0 & 0 & \mathbb{L} \end{pmatrix} \begin{pmatrix} \mathbb{I} & 0 & (\mathbb{K}_i^{\Omega})^{-1}\mathbb{K}_i^{\Omega,\Sigma} \\ 0 & \mathbb{I} & (\mathbb{K}_j^{\Omega})^{-1}\mathbb{K}_j^{\Omega,\Sigma} \\ 0 & 0 & \mathbb{I} \end{pmatrix},$$

The Schur complement $\mathbb{L} = \mathbb{L}_i + \mathbb{L}_j$ is dense $\Leftrightarrow$ discrete DtN map
$\rightarrow$ advances on dense Block Low-Rank factorization [*Amestoy et al. 2019*]

The non-overlapping Schwarz approach can be seen as an iterative solver for $\mathbb{L}$ preconditioned by interfaces conditions
$\rightarrow$ approximate block LU factorization at the continuous level

Outline

Summary and updated objective

Non-overlapping domain decomposition for flow acoustics

- similar to the Helmholtz formulation, common framework
- quick convergence relies on sparse approximations of the DtN map
  $\Leftrightarrow$ Non-reflecting boundary conditions

Summary and updated objective

Non-overlapping domain decomposition for flow acoustics

- similar to the Helmholtz formulation, common framework
- quick convergence relies on sparse approximations of the DtN map
  $\Leftrightarrow$ Non-reflecting boundary conditions

Updated objective

Design non-reflecting boundary conditions for heterogeneous and convected time-harmonic problems

Two techniques were studied during the thesis

1. Absorbing Boundary Conditions (ABC) [*Marchner et al. SIAP 2022*],
2. Perfectly Matched Layers (PML) [*Marchner et al. JCP 2021*],

Summary and updated objective

Non-overlapping domain decomposition for flow acoustics

- similar to the Helmholtz formulation, common framework
- quick convergence relies on sparse approximations of the DtN map
  $\Leftrightarrow$ Non-reflecting boundary conditions

Updated objective

Design non-reflecting boundary conditions for heterogeneous and convected time-harmonic problems

Two techniques were studied during the thesis

1. Absorbing Boundary Conditions (ABC) [*Marchner et al. SIAP 2022*],
2. Perfectly Matched Layers (PML) [*Marchner et al. JCP 2021*],

Next section

Focus on the construction of Absorbing Boundary Conditions

Outline

Outline

Microlocal analysis - DtN operator

Goal: find local approximations to the **Dirichlet-to-Neumann map**

DtN operator on Σ

$$\widetilde{\Lambda^+} : \begin{cases} H^{1/2}(\Sigma) \to H^{-1/2}(\Sigma) \\ u_{|\Sigma} \mapsto \partial_{\boldsymbol{n}} u_{|\Sigma} = -i\widetilde{\Lambda^+} u_{|\Sigma} \end{cases}$$

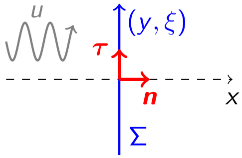

through pseudo-differential calculus

[*Engquist and Majda 1977, 1979*] [*Antoine et al. 1999*]

Example : 2D heterogeneous Helmholtz half-space problem

$$\mathcal{L} = \rho_0^{-1}\partial_x(\rho_0\partial_x) + \rho_0^{-1}\partial_y(\rho_0\partial_y) + \omega^2 c_0^{-2}$$
$$\underset{?}{\approx} \left(\partial_x + \imath\sqrt{\omega^2 c_0^{-2} + \rho_0^{-1}\partial_y(\rho_0\partial_y)}\right)\left(\partial_x - \imath\sqrt{\omega^2 c_0^{-2} + \rho_0^{-1}\partial_y(\rho_0\partial_y)}\right)$$

We cannot formally factorize $\mathcal{L}$ when $\partial_x(\rho_0) \neq 0$ or $\partial_x(c_0) \neq 0$

- Apply the principle to the **symbol** λ^+ of Λ^+

$\rightarrow$ work on polynomials in the co-tangent Fourier space ξ

Pseudo-differential operator

We define a differential operator of order m,

$$\mathcal{P}(\boldsymbol{x}, \partial_{\boldsymbol{x}}) = \sum_{|\boldsymbol{\alpha}| \leq m} (-\imath)^{\boldsymbol{\alpha}} a_{\boldsymbol{\alpha}}(\boldsymbol{x}) \partial_{\boldsymbol{x}}^{\boldsymbol{\alpha}}, \quad x \in \mathbb{R}^d, \ \boldsymbol{\alpha} = (\alpha_1, \ldots, \alpha_d) \in \mathbb{N}^d,$$

through its inverse Fourier representation $\rightarrow$ more general framework

Pseudo-differential operator of order m

$$\mathcal{P}(\boldsymbol{x}, \partial_{\boldsymbol{x}}) u(\boldsymbol{x}) = \frac{1}{(2\pi)^d} \int_{\mathbb{R}^d} e^{\imath \boldsymbol{x} \cdot \boldsymbol{\xi}} p(\boldsymbol{x}, \boldsymbol{\xi}) \hat{u}(\boldsymbol{\xi}) d\boldsymbol{\xi}, \ \boldsymbol{\xi} \in \mathbb{R}^d$$

p is the symbol of the operator $\mathcal{P}$, and is a smooth function of $(\boldsymbol{x}, \boldsymbol{\xi})$

Symbol of the operator $\mathcal{P}$

$$p(\boldsymbol{x}, \boldsymbol{\xi}) = \sum_{|\boldsymbol{\alpha}| \leq m} a_{\boldsymbol{\alpha}}(\boldsymbol{x}) \boldsymbol{\xi}^{\boldsymbol{\alpha}}, \quad \boldsymbol{\xi}^{\boldsymbol{\alpha}} = \xi_1^{\alpha_1} \ldots \xi_d^{\alpha_d}$$

The highest order term is the principal symbol. We use **classical symbols** $\mathcal{S}_{\text{cl}}^m$

$$\left| \partial_{\boldsymbol{x}}^{\boldsymbol{\beta}} \partial_{\boldsymbol{\xi}}^{\boldsymbol{\alpha}} p(\boldsymbol{x}, \boldsymbol{\xi}) \right| \leq C(\boldsymbol{\alpha}, \boldsymbol{\beta}, K)(1 + |\boldsymbol{\xi}|)^{m - |\boldsymbol{\alpha}|}, \quad \forall (\boldsymbol{x}, \boldsymbol{\xi}) \in K \times \mathbb{R}^d,$$

Notations:

$\mathcal{P} = \text{Op}(p) \in \text{OPS}^m, \quad p \in \mathcal{S}_{\text{cl}}^m \Leftrightarrow \mathcal{P} \in \text{OPS}^m, \quad \text{OPS}^{-\infty} = \bigcap_{m \in \mathbb{R}} \text{OPS}^m$

Derivation of the DtN symbol - Helmholtz case

Nirenberg's factorization theorem: there exists $(\Lambda^+, \Lambda^-) \in \mathrm{OPS}^1$

$$\mathcal{L} = \left(\partial_x + \imath\Lambda^-\right)\left(\partial_x + \imath\Lambda^+\right) \quad \text{mod OPS}^{-\infty}$$
$$= \partial_x^2 + \imath\left(\Lambda^+ + \Lambda^-\right)\partial_x + \imath\mathrm{Op}\left\{\partial_x\lambda^+\right\} - \Lambda^-\Lambda^+ \quad \text{mod OPS}^{-\infty}.$$

Identify with the Helmholtz operator and get a system for (Λ^+, Λ^-)

$$\begin{cases} \Lambda^+ + \Lambda^- = -\imath\rho_0^{-1}\partial_x(\rho_0) \\ \left(\Lambda^+\right)^2 + \imath\rho_0^{-1}\partial_x(\rho_0)\Lambda^+ + \imath\mathrm{Op}\left\{\partial_x\lambda^+\right\} = \omega^2 c_0^{-2} + \rho_0^{-1}\partial_y(\rho_0\partial_y) \end{cases}$$

$\rightarrow$ "One-way" reformulation of the equation
"High frequency" asymptotic expansion for the total symbol λ^+

$$\lambda^+ \sim \sum_{j=-1}^{\infty} \lambda_{-j}^+ = \lambda_1^+ + \lambda_0^+ + \lambda_{-1}^+ + \cdots \text{ (classical symbol expansion)}$$

Each symbol λ_{-j}^+ is homogeneous in $(\omega, \xi)^{-j}$.
Once λ_1^+ is fixed, the expansion is unique and can computed formally

$$\lambda_1^+ = \sqrt{\omega^2 c_0^{-2} - \xi^2}, \; \lambda_0^+ = -\imath\left(\frac{\partial_x(\rho_0)}{2\rho_0} + \frac{\xi\partial_y(\rho_0)}{2\rho_0\lambda_1^+} + \frac{\omega^2\partial_x\left(c_0^{-2}\right)}{4\left(\lambda_1^+\right)^2} + \frac{\xi\omega^2\partial_y\left(c_0^{-2}\right)}{4\left(\lambda_1^+\right)^3}\right)$$

Microlocal zones

Hyperbolic zone: $\Re(\lambda_1^+) > 0 \rightarrow$ outgoing propagative waves
Elliptic zone: $\Im(\lambda_1^+) < 0 \rightarrow$ outgoing evanescent waves

Rotation of the square-root branch-cut [*Milinazzo et al. 1997*]

$$\lambda_1^+ = e^{\imath\alpha/2}\sqrt{e^{-\imath\alpha}(\omega^2 c_0^{-2} - \xi^2)},\ \alpha \in [0, -\pi],\ (+\imath\omega t \text{ convention})$$

The branch-cut is rotated by an angle α in the complex plane

- Hyperbolic zone: $\omega c_0^{-1} > |\xi| \rightarrow \alpha = 0$,
- Elliptic zone: $\omega c_0^{-1} < |\xi| \rightarrow \alpha = -\pi$,
- Grazing zone: $\omega c_0^{-1} = |\xi|$, ill-posed problem

In practice we choose $\alpha \in (0, -\pi/2]$
$\rightarrow$ trade-off to capture both propagative and evanescent waves

Summary - building the DtN approximation

Approximate DtN operator with the M first symbols

$$\partial_{\mathbf{n}} u = -\imath \Lambda_M^+ u, \quad \Lambda_M^+ = \sum_{j=-1}^{M-2} \mathrm{Op}\left(\lambda_{-j}^+\right)$$

Take the trace on the boundary Σ to get $\widetilde{\Lambda}_M^+$, such that

$$\left(\widetilde{\Lambda}^+ - \widetilde{\Lambda}_M^+\right) \in \mathsf{OPS}^{1-M}$$

Technical difficulties

- the formal computation of λ_{-j}^+ can be involved (PDE dependent)
- the operator $\mathrm{Op}\left(\lambda_{-j}^+\right)$ is in general not unique and still non-local
- limited *a priori* to smooth variations of ρ_0 and c_0

Next step - original contribution

- Apply the theory to flow acoustics

Outline

DtN symbol computation

Step 1 Nirenberg's factorization theorem for the flow acoustics operator

$$\mathcal{L} = \frac{D_0}{Dt}\left(\frac{1}{c_0^2}\frac{D_0}{Dt}\right) - \rho_0^{-1}\nabla\cdot\left(\rho_0\nabla\right), \quad \frac{D_0}{Dt} = \imath\omega + \mathbf{v}_0\cdot\nabla$$

We note $M_x = v_{0,x}/c_0$, $M_y = v_{0,y}/c_0$, $\mathrm{M} = \left\|\mathbf{v}_0\right\|/c_0$, $k_0 = \omega/c_0$

Step 2 Derive an operator equation for the outgoing characteristic Λ^+

$$\left(1 - {M_x}^2\right)(\Lambda^+)^2 - \imath\left(\mathcal{A}_1 + \mathcal{A}_0\right)\Lambda^+ + \imath(1 - {M_x}^2)\mathrm{Op}\left\{\partial_x\lambda^+\right\} = \mathcal{B}_2 + \mathcal{B}_1 \mod \mathrm{OPS}^{-\infty}$$

with $\imath\left(\Lambda^+ + \Lambda^-\right) = \left(\mathcal{A}_1 + \mathcal{A}_0\right)/({M_x}^2 - 1)$, $\sigma(\mathcal{A}_j), \sigma(\mathcal{B}_j) \in \mathcal{S}^j_{\mathrm{cl}}$, $j = \{0, 1, 2\}$

Step 3 Classical symbol expansion, identify 2nd order terms in (ω, ξ)

DtN principal symbol for flow acoustics

$$\lambda_1^{\pm} = \frac{1}{1-{M_x}^2}\left[-M_x\left(k_0 - \xi M_y\right) \pm \sqrt{k_0^2 - 2k_0 M_y\xi - \left(1 - \mathrm{M}^2\right)\xi^2}\right]$$

Microlocal zones delimited by $\omega c_0^{-1} = \left(M_y \pm \sqrt{1 - {M_x}^2}\right)\xi$

Subsonic flow $\mathrm{M} < 1 \Rightarrow$ two characteristic lines of opposite sign

DtN symbol computation

Step 3 - bis
Compute the next symbols of the expansion ...

$$\lambda_0^+ = \frac{\sigma(\mathcal{B}_1) + i\sigma(\mathcal{A}_0)\lambda_1^+ + i(1 - {M_x}^2)\left(\partial_\xi \lambda_1^+ \partial_y \lambda_1^+ - \partial_x \lambda_1^+\right)}{2\sqrt{k_0^2 - 2k_0 M_y \xi - (1 - \mathrm{M}^2)\,\xi^2}}.$$

If $M_y = 0$ we have the simplification

Zeroth order symbol for an x-oriented flow

$$\lambda_0^+ = -\imath \frac{\partial_x(\rho_0)}{2\rho_0} \frac{k_0^2 - \xi^2}{k_0^2 - (1 - {M_x}^2)\xi^2} + \imath \frac{\partial_x(c_0)}{2c_0} \frac{k_0^2 + {M_x}^2 \xi^2}{k_0^2 - (1 - {M_x}^2)\xi^2}$$

$$\lambda_{-1}^+ = ..., \quad \lambda_{-2}^+ = ...$$

Going back to the operator level

Final step go back to the operator level

Approximate DtN operator

$$\widetilde{\Lambda}_1^+ = \mathrm{Op}(\lambda_1^+) = \frac{k_0}{1-M_{\boldsymbol{n}}^2}\left(-M_{\boldsymbol{n}} + \imath M_{\boldsymbol{n}} M_{\boldsymbol{\tau}} \frac{\nabla_\Sigma}{k_0} + \sqrt{1+X}\right)$$

$$X = -2\imath M_{\boldsymbol{\tau}} \frac{\nabla_\Sigma}{k_0} + \left(1 - \mathrm{M}^2\right)\frac{\Delta_\Sigma}{k_0^2}, \quad \mathrm{M} = \|\mathbf{v}_0\| / c_0$$

For the half-space problem with constant coefficients

$$\widetilde{\Lambda}^+ = \widetilde{\Lambda}_1^+ \quad \mathrm{mod}\ \mathrm{OPS}^{-\infty}$$

For variable coefficients and/or in the tangent plane approximation $(\boldsymbol{n}, \boldsymbol{\tau})$

$$\widetilde{\Lambda}^+ = \widetilde{\Lambda}_1^+ \quad \mathrm{mod}\ \mathrm{OPS}^{0}$$

The choice for $\mathrm{Op}(\lambda_1^+)$ is not unique, but has λ_1^+ as principal symbol

Issue: the approximate DtN map $\widetilde{\Lambda}_1^+$ is still non-local
$\rightarrow$ we need a local representation for $\sqrt{1+X}$

Localization procedure

High-frequency approximation for $\sqrt{1+X}$, $X \to 0$ $(\omega \to +\infty)$
Use complexified Padé or Taylor approximations (N, α) for

$$\Lambda(Z) = e^{\imath\alpha/2}\sqrt{1+Z}, \quad Z = [e^{-\imath\alpha}(1+X) - 1],$$

with Z a surfacic second order differential operator on the boundary Σ

Taylor approximation

$$\Lambda(Z) \approx e^{\imath\alpha/2} \sum_{\ell=0}^{N} \binom{1/2}{\ell} \left(e^{-\imath\alpha}(1+X) - 1\right)^{\ell}$$

Padé approximation

$$\Lambda(Z) \approx K_0(\alpha) + \sum_{\ell=1}^{N} A_\ell(\alpha) X (1 + B_\ell(\alpha) X)^{-1}$$

Resulting local Absorbing Boundary Conditions

Complex Padé approximants: $\widetilde{\Lambda}_1^+ \to \mathrm{ABC}_1^{N,\alpha}$

Complex Taylor approximants: $\widetilde{\Lambda}_1^+ \to \mathrm{ABC}_1^{\mathrm{T0},\alpha}$ and $\mathrm{ABC}_1^{\mathrm{T2},\alpha}$

High-order FEM implementation

Discretization on a conformal, high-order H^1-basis

Weak formulation for the linearized potential equation

$\forall v \in V \subseteq H^1(\Omega)$,

$$\int_\Omega \left[\rho_0 \nabla u \cdot \overline{\nabla v} - \frac{\rho_0}{c_0^2} \frac{D_0 u}{Dt} \overline{\frac{D_0 v}{Dt}}\right] d\Omega + \imath \int_\Sigma \mathcal{G} u \bar{v} \, d\Sigma = \int_\Omega f \bar{v} d\Omega$$

The boundary operator $\mathcal{G}$ takes the same form as in the Helmholtz case

$$\int_\Sigma \mathcal{G} u \, \bar{v} \, d\Sigma = \int_\Sigma e^{\imath\alpha/2} \rho_0 k_0 \sqrt{1 + Z} \, u \, \bar{v} \, d\Sigma$$

with $Z = e^{-\imath\alpha} \left(1 - 2\imath M_\tau \frac{\nabla_\Sigma}{k_0} + \left(1 - \mathrm{M}^2\right) \frac{\Delta_\Sigma}{k_0^2}\right) - 1$

High-order FEM implementation

Discretization on a conformal, high-order H^1-basis

Weak formulation for the linearized potential equation

$\forall v \in V \subseteq H^1(\Omega)$,

$$\int_\Omega \left[\rho_0 \nabla u \cdot \overline{\nabla v} - \frac{\rho_0}{c_0^2}\frac{D_0 u}{Dt}\overline{\frac{D_0 v}{Dt}}\right] d\Omega + \imath \int_\Sigma \mathcal{G} u \overline{v}\, d\Sigma = \int_\Omega f \overline{v} d\Omega$$

The boundary operator $\mathcal{G}$ takes the same form as in the Helmholtz case

$$\int_\Sigma \mathcal{G} u\, \overline{v}\, d\Sigma = \int_\Sigma e^{\imath\alpha/2} \rho_0 k_0 \sqrt{1+Z}\, u\, \overline{v}\, d\Sigma$$

with $Z = e^{-\imath\alpha}\left(1 - 2\imath M_\tau \frac{\nabla_\Sigma}{k_0} + \left(1-\mathrm{M}^2\right)\frac{\Delta_\Sigma}{k_0^2}\right) - 1$

Taylor approximants: $\mathrm{ABC}_1^{\mathrm{T2},\alpha}$

$$\int_\Sigma \mathcal{G} u\, \overline{v}\, d\Sigma = \cos(\alpha/2) \int_\Sigma \rho_0 k_0\, u\, \overline{v}\, d\Sigma + e^{-\imath\alpha/2}\left(\int_\Sigma \rho_0 M_\tau \nabla_\Sigma u\, \overline{v}\, d\Sigma - \int_\Sigma \rho_0 \frac{(1-\mathrm{M}^2)}{2k_0} \nabla_\Sigma u\, \nabla_\Sigma \overline{v}\, d\Sigma\right)$$

High-order FEM implementation - Padé case

Padé approximants: $\mathrm{ABC}_1^{N,\alpha}$

$$\int_\Sigma \mathcal{G} u \, \overline{v} \, d\Sigma = \int_\Sigma \rho_0 k_0 K_0(\alpha) \, u \, \overline{v} \, d\Sigma + \sum_{\ell=1}^{N} \int_\Sigma \rho_0 k_0 A_\ell(\alpha) \, X \varphi_\ell \, \overline{v} \, d\Sigma$$

with $X = -2\imath M_\tau \frac{\nabla_\Sigma}{k_0} + \left(1 - \mathrm{M}^2\right) \frac{\Delta_\Sigma}{k_0^2}$

Introduce **auxiliary fields** $\varphi_\ell = (1 + B_\ell X)^{-1} u$ to obtain a **sparse** discretization of inverse operators
$\rightarrow$ augmented system of N surfacic equations

$$\forall \ell \in [1, N], \ \forall v_\ell \in H^1(\Sigma)^N, \quad \int_\Sigma (1 + B_\ell(\alpha) X) \varphi_\ell \overline{v}_\ell \, d\Sigma = \int_\Sigma u \overline{v}_\ell \, d\Sigma$$

Global linear system of size $[N_{\mathrm{dof},\Omega} + (N \times N_{\mathrm{dof},\Sigma})]$

Outline

Longitudinal heterogeneous waveguide

Example 1: No mean flow, single mode propagation in a heterogeneous waveguide: $\rho_0 = 1,\ c_0(x,y) = c_0(x)$

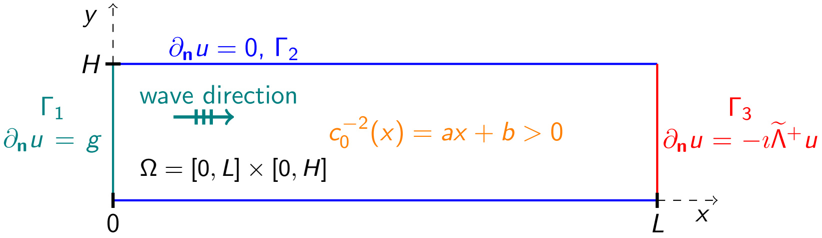

Single mode analytic solution for a linear profile

$$u_{\mathrm{ex}}^n(x,y) = \cos(k_y y)\,\mathrm{Ai}\left(e^{-\frac{2\imath\pi}{3}}\frac{k_y^2 - \omega^2(ax+b)}{(a\omega^2)^{2/3}}\right), \quad k_y = \frac{n\pi}{H}, \quad n \in \mathbb{N}$$

Approximation at the symbol level

$c_0^{-2}(x) = 5x + 0.1$, $L = 1$ at fixed frequency $\omega = 30$

Analytic total symbol

$$\lambda^+ = -\imath e^{-\frac{2\imath\pi}{3}} \left(a\omega^2\right)^{1/3} \frac{\mathrm{Ai}'(\zeta)}{\mathrm{Ai}(\zeta)}, \quad \zeta = e^{-\frac{2\imath\pi}{3}} \frac{\xi^2 - \omega^2(aL+b)}{(a\omega^2)^{2/3}}$$

$$\left|\lambda^+ - \sum_{j=-1}^{M-2} \lambda^+_{-j}\right|$$

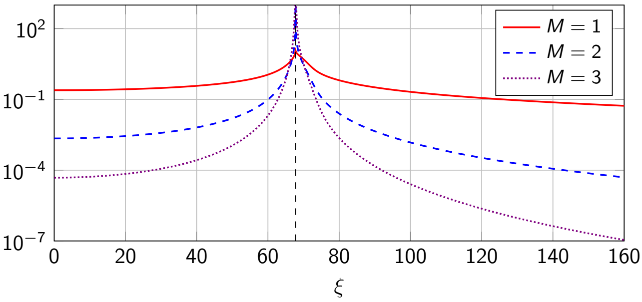

- singularity in the grazing regime $\xi \approx \omega c_0^{-1}$

$ABC_M^{N,\alpha}$: Local Padé approximation of $\widetilde{\Lambda}_M^+$ with rotation branch-cut α

$\omega = 20,\ x_t = 0.16,\ n = 3$

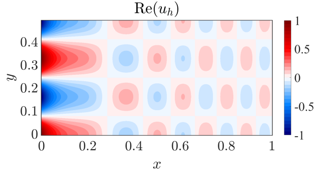

Relative L^2-error (%)

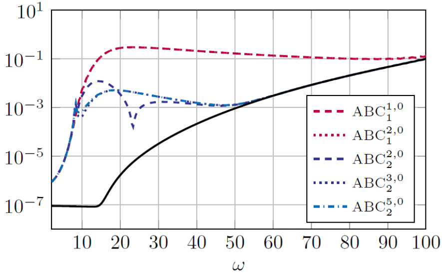

Use the derivative of c_0 $\Rightarrow$ more accurate ABC: $ABC_2^{N+1,\alpha} > ABC_1^{N,\alpha}$

Gain of $\approx$ two order of magnitude
Precision limited by the DtN symbol truncation

Similar conclusion with Taylor approximations of order 0 and 2

Example 2: $\rho_0 = c_0 = 1$, point source in uniform mean flow of angle θ

Padé approximants $\to$ $\text{ABC}_1^{N,\alpha}$, Taylor approximants $\to$ $\text{ABC}_1^{\text{T0},\alpha}$, $\text{ABC}_1^{\text{T2},\alpha}$

Attempt to incorporate curvature effects from λ_0^+ (circle of radius R)

$$\text{ABC}_2 = \text{ABC}_1 + (1 - \text{M}^2)/(2R)$$

$k_0 = 6\pi, \text{M} = 0.95, R = 1, \theta = \pi/4$

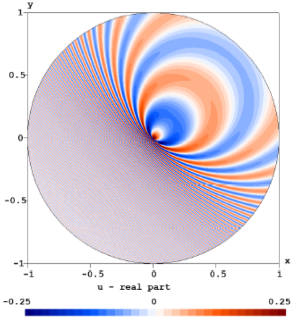

Relative L^2-error (%)

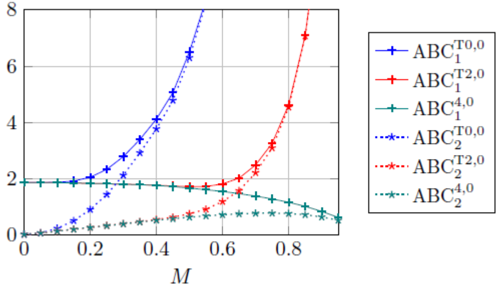

$\text{ABC}_1^{N,\alpha}$ is robust for high Mach numbers - wavelength ratio $(1 + \text{M})/(1 - \text{M})$

Outline

Outline

Waveguide problem with straight partitions

Domain partition: $\Omega = \bigcup_{i=0}^{N_{\text{dom}}-1} \Omega_i,\ \Sigma_{ij} = \overline{\partial\Omega_i \bigcap \partial\Omega_j},\ j \neq i$

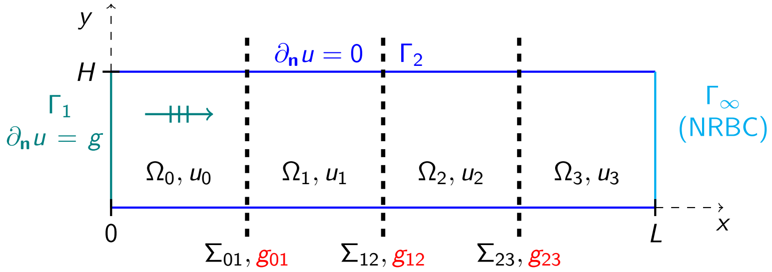

Two test cases

1. Linear speed of sound profile : $c_0^{-2}(x) = ax + b$
2. Transverse density and/or speed of sound : $c_0(y), \rho_0(y)$

Reminder - ABC study

- $\text{ABC}_2^{N+1,\alpha} > \text{ABC}_1^{N,\alpha}$
- Precision limited by the truncation of the total DtN symbol λ^+

Plot theoretical convergence radius $\rho(m,x) = \sqrt{\left|\mathcal{T}_{ij}^m \mathcal{T}_{ji}^m\right|}$ at $\omega = 30$

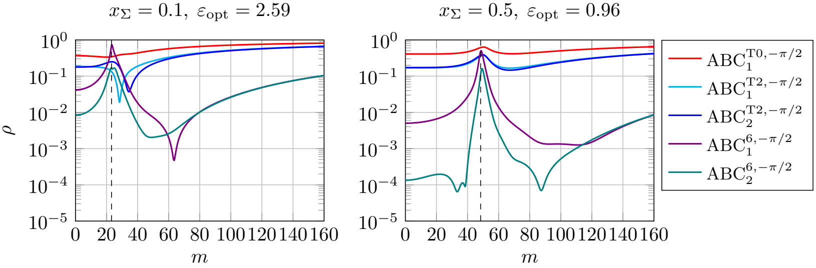

DDM waveguide study - input boundary condition with the 21 first modes

N_{dom}	$\text{ABC}_1^{\text{T0},\alpha}$	$\text{ABC}_1^{\text{T2},\alpha}$	$\text{ABC}_1^{6,\alpha}$	$\text{ABC}_2^{6,\alpha}$
8	76 (dnc)	51 (87)	34 (37)	24 (27)

Table: GMRES(Jacobi) iterations to 10^{-6} at $\omega = 40, \alpha = -\pi/4, d_\lambda = 12$

Transverse heterogeneous waveguide

Gaussian waveguide: $c_0(y) = 1.25\left(1 - 0.4e^{-32(y-H/2)^2}\right), \rho_0(y) = c_0^2(y)$

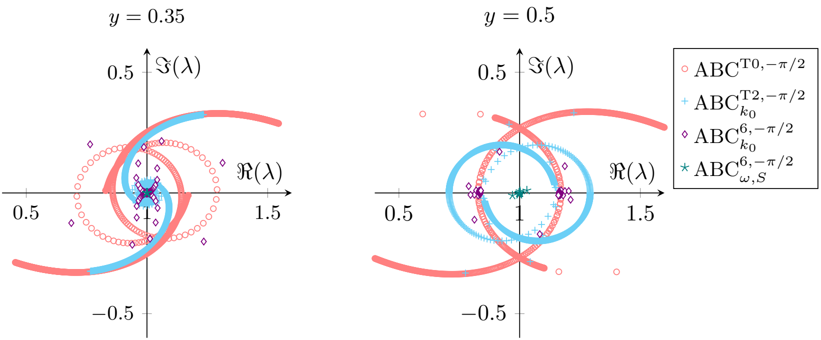

Figure: Theoretical eigenvalues of the DDM iteration matrix, $\omega = 50$

- Usual Padé approximation (classical principal symbol) - $\mathcal{S}_i = \mathrm{ABC}_{k_0}^{N,\alpha}$
- New approximation (semi-classical principal symbol) - $\mathcal{S}_i = \mathrm{ABC}_{\omega,S}^{N,\alpha}$
  $\rightarrow$ almost perfect clustering

DDM - large PML on Γ_∞ - input mode $n = 4$ - $N_{\text{dom}} = 8$

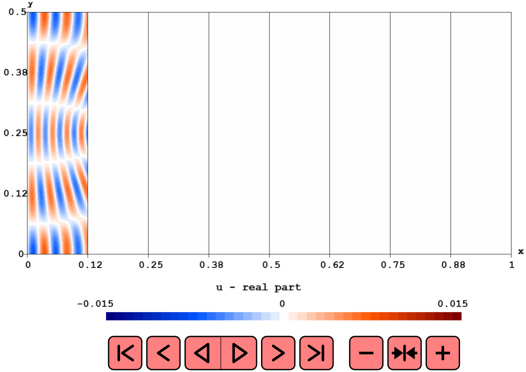

N_{dom}	$\text{ABC}_{k_0}^{\text{T0},-\pi/4}$	$\text{ABC}_{k_0}^{\text{T2},-\pi/4}$	$\text{ABC}_{k_0}^{4(8),-\pi/4}$	$\text{ABC}_{\omega}^{4(8),-\pi/4}$
8	111	74	42 (42)	20 (8)

Table: GMRES iterations to 10^{-6} at $\omega = 160$, $d_\lambda = 24$

Convergence in N_{dom} iterations $\rightarrow$ continuous block LU factorization

Outline

Convected problem in freefield - circular interfaces

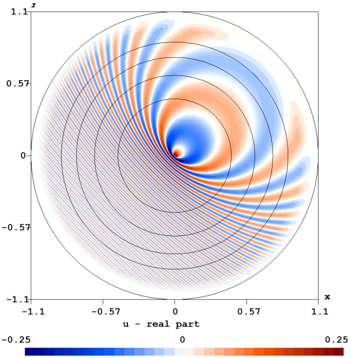

(a) $\mathrm{ABC}_1^{4,-\pi/4}$, $\mathcal{E}_{L^2} = 1.7\%$

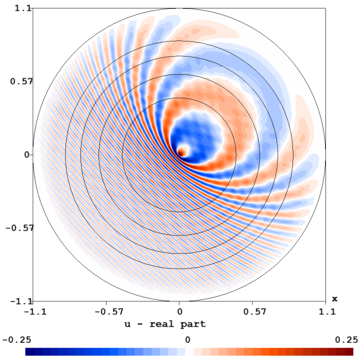

(b) $\mathrm{ABC}_1^{T2,-\pi/4}$, $\mathcal{E}_{L^2} = 24\%$

Numerical solution after 4 GMRES iterations.
Parameters: $\mathrm{M} = 0.9,\ \theta = \pi/4,\ p = 9,\ d_\lambda = 8,\ N_{\mathrm{dom}} = 5,\ \omega = 6\pi$.
L^2-error "PML-analytical solution" : 0.8%.

Padé conditions are robust for **high Mach numbers**

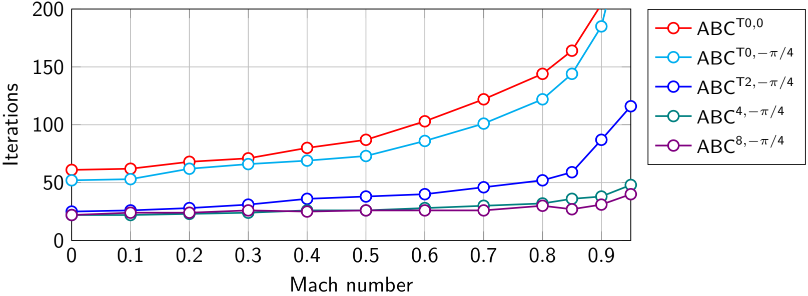

Figure: GMRES iterations to reach 10^{-6} for $N_{\text{dom}} = 5$, $\omega = 6\pi$

- Only Padé conditions are robust for high Mach numbers
- Layered partition: iteration number increases as $\mathcal{O}(N_{\text{dom}})$

Convected problem in freefield - arbitrary decomposition

$N_{\text{dom}} = 256$

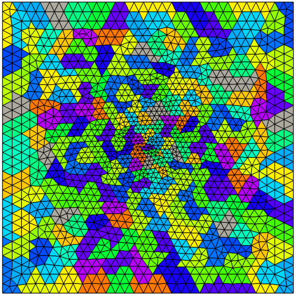

Automatic partitioning

- Cross-points
  $\rightarrow$ harder to design ABCs
- Industrial need - good load balancing between subproblems
- Shorter connectivity graph - $\mathcal{O}(\sqrt{N_{\text{dom}}})$

Corner problem : use Padé approximants on edges with Sommerfeld-type condition on corners $\rightarrow$ approximate corner treatment
Resulting condition $\text{ABC}_S^{N,\alpha}$

Are such Padé conditions still effective for domain decomposition ?

Numerical study - arbitrary decomposition

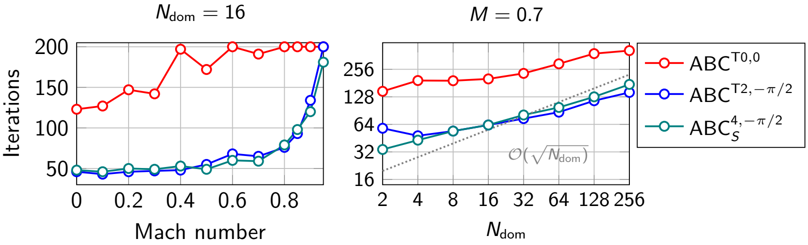

GMRES iterations to reach 10^{-6} for $\omega = 6\pi, d_\lambda = 8$

- lost of robustness for high Mach numbers
- $ABC^{T2,-\pi/2}$, $ABC_S^{4,-\pi/2}$ $\rightarrow$ similar performance
- $ABC^{T2,-\pi/2}$ is cheaper (and easier) to implement

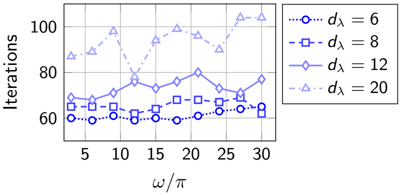

$M = 0.7$, $N_{dom} = 16$, $ABC^{T2,-\pi/2}$

Outline

The boundary value problem

Given a flight configuration (mean flow), predict the radiated noise from the fan, at multiples of the blade passing frequency $\omega_{\mathsf{bpf}}/(2\pi) = 1300$ Hz

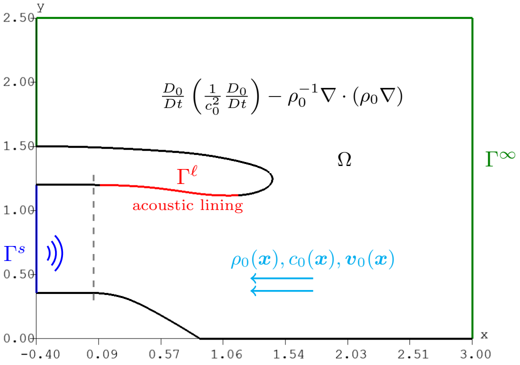

Boundary conditions

- Ingard-Myers on Γ_ℓ
- PML (active) on Γ^s
- Fixed annular Bessel mode on Γ^s
- PML (passive) on Γ^∞

The mean flow is pre-computed and **interpolated** on the acoustic mesh

Outline

DDM for the 3D turbofan problem

ω_{bpf} - $N_{\text{dofs}} = 10\text{M}$ - nnz$= 730\text{M}$ $\approx$ 25 wavelengths in Ω

Direct solver $\rightarrow$ 740 Gb RAM for factorization

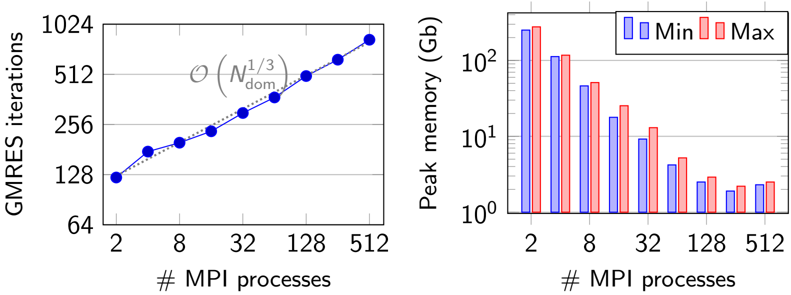

Parallel GmshDDM solver (mono-thread)

From $N_{\text{dom}} > 128$, under 10 minutes and less than 3Gb per process

Iterations for $N_{\text{dom}} = 64$

- $\text{ABC}^{\text{T2},-\pi/2}$: 372 GMRES iterations to 10^{-6}
- $\text{ABC}^{\text{T0},0}$: $>$ 2000 GMRES iterations to reach 10^{-3}

DDM for the 3D turbofan problem

$2 \times \omega_{\text{bpf}}$ - $N_{\text{dofs}} = 73\text{M}$ - nnz $= 5\text{B}$ $\approx$ 50 wavelengths in Ω

Parallel GmshDDM solver (mono-thread), $N_{\text{dom}} = \#$ MPI $= 128$

$\rightarrow$ 2hours 3min, 26 Gb peak memory, 712 GMRES iterations (with lining)

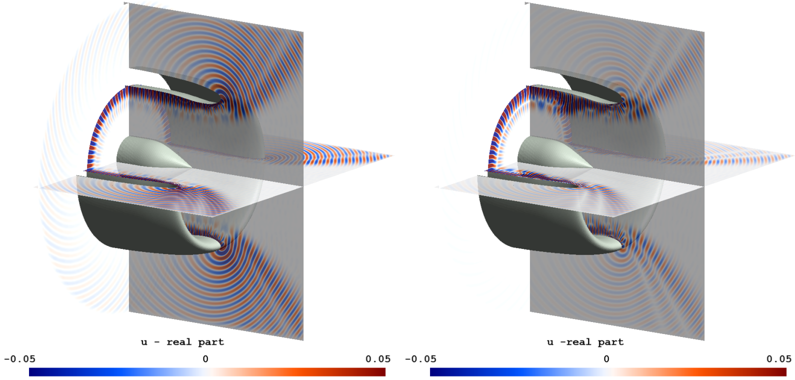

Figure: Real part of the acoustic velocity potential for the mode $(48, 1)$ at $2 \times \omega_{\text{bpf}}$ (2600 Hz) without (left) and with (right) acoustic lining treatment.

Outline

Weak scalability assessment

3D Helmholtz problem with $d_\lambda = 7.5$ points per wavelength

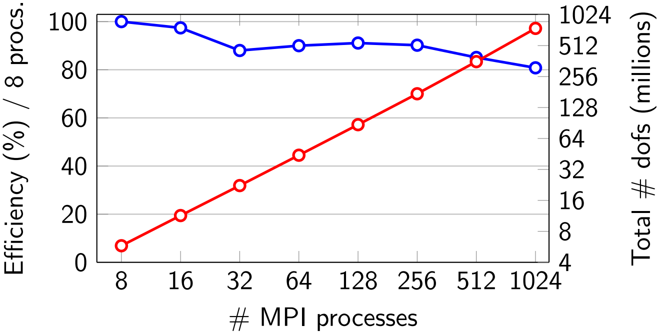

Figure: Weak scaling timing for 1 iteration

Limitations

- memory load balancing: [20-34] Gb for 1024 processes
- number of iterations scales as $\mathcal{O}(N_{\text{dom}}^{1/3})$ in 3D

General summary and conclusion

Distributed memory solver for high frequency flow acoustics

1. Extension of a generic domain decomposition method to flow acoustics
2. Development of non-reflecting boundary conditions: ABCs and PMLs
   - extension to media with heterogeneities and convection
   - general PML procedure for flow acoustics
3. Code development (`GmshDDM`), validation and assessment of ABCs in a domain decomposition context
4. Proof of concept - turbofan intake
5. 80% scalability up to 700M high-order unknowns and 1024 MPI processes

General summary and conclusion

Limitations

- The iterative solver does not scale with $N_{\text{dom}} \rightarrow$ requires coarse space
- Theoretical limitations - corners, curved boundaries, PML-DDM, etc.

Future developments

- Extension to Pierce equation $\rightarrow$ turbofan exhaust [*Spieser, Bailly 2020*]
- Modern discretization techniques such as HDG or HHO [*Li et al. 2013*]
- Interfaces through the mesh $\rightarrow$ immersed transmission conditions

General summary and conclusion

Limitations

- The iterative solver does not scale with $N_{\text{dom}} \rightarrow$ requires coarse space
- Theoretical limitations - corners, curved boundaries, PML-DDM, etc.

Future developments

- Extension to Pierce equation $\rightarrow$ turbofan exhaust [*Spieser, Bailly 2020*]
- Modern discretization techniques such as HDG or HHO [*Li et al. 2013*]
- Interfaces through the mesh $\rightarrow$ immersed transmission conditions

Thank you !